Automated Computational Diagnosis of Peripheral Retinal Pathology in Optical Coherence Tomography (OCT) Scans using Graph Theory

Tyra Lange, Stewart Lake, Karen Reynolds, Murk Bottema

***Abstract*— Analysis of retinal shape with optical coherence tomography (OCT) has been valuable in describing different ophthalmic conditions. An effective method for retinal contour delineation is graph theory. This study compares the ability of two different implementations of graph theory, the Livewire (LVW) intelligent scissors developed for ImageJ and a purpose-built graph searching function (GSF), to determine retinal shape for a retinal disease classifier. Both methods require user interaction. Retinal shape features derived from both methods were used to diagnose eyes with posterior vitreous detachment (PVD) or retinal detachment (RD) via quadratic discriminant analysis. Classification with each method was the same in 49 out of 51 eyes. Processing time was faster with the GSF than LVW. In mean (μ) ± standard deviation (SD), GSF took 524 ± 62 s and LVW took 814 ± 223 s ($p = 5.52 \times 10^{-14}$). Conclusively, GSF was easier to use and is preferred for further retinal shape analysis.**

Keywords*— Optical coherence tomography (OCT), computational diagnosis, retinal pathology, graph theory

I. Introduction

OCT is an in vivo imaging modality, which rapidly acquires high-resolution cross-sectional images of biological tissue, using the backscatter of low-coherence light from a super luminescent diode [1]. These high-resolution images have become an established medical tool for the diagnosis of retinal pathology and a fundamental resource in ophthalmic research. OCT interferometric sensitivity and spectral transmission properties of ocular tissues facilitates viewing of the layered structure of the retina with a 10 μm depth resolution [1]. Thus, OCT can be employed to investigate individual subretinal layers. Retinal segmentation into subretinal layers in OCT images, or B-scans, has enabled the quantification of the degree of retinal curvature, a key indicator of PVD and RD [2].

Whilst technological improvements continue in the OCT image acquisition system, retinal layer segmentation can be time-consuming, inefficient and onerous. Additionally, manual extraction methods are susceptible to subjective bias and are expertise dependent. Current software used to perform automated data-acquisition, processing, and displaying of OCT images is subject to proprietary ownership. The publication of segmentation algorithms such as the IOWA Reference Algorithms [3], the Graph-Based Segmentation [4] software and the Retina Segmentation Toolbox [5], has facilitated a degree of access however, open segmentation remains largely inaccessible to most clinicians and researchers. Therefore, there is need for an image analysis tool that accurately delineates retinal layers.

A semi-automated, highly accurate and consistent method that quantifies retinal curvature could be used to parameterise pathology for large-scale clinical studies into the assessment, monitoring, as well as early detection of retinal lesions. Evident within current research is the active development and testing of image analysis algorithms employing intensity thresholding [6], active-contours [7], machine learning [8] and graph theory [9], which has resulted in quantified descriptions of healthy retinae, however large areas of automated diagnosis still remain unexplored. The aims of this study were twofold:

1. To design and implement a GSF in MATLAB, which utilises graph theory and Dijkstra's minimum weighted path method, to delineate retinal morphology within each B-scan in a 3D-OCT cube.
2. To compare shape metrics from the GSF to those from the LVW intelligent scissors developed for ImageJ. Comparison was made based on image processing time, and performance of a discriminant analysis classifier based on derived shape features.

II. Image Acquisition

A. Clinical Study

Images were obtained at Flinders Ophthalmology, Adelaide. The study was undertaken with institutional review board approval, in accordance with the Declaration of Helsinki. Two OCT cubes from 51 eyes (n=51) of 31 participants were included. Within the dataset, 28 eyes had a diagnostic category (either PVD or RD) whilst the remaining 23 eyes were part of a predictive study of classifier performance with no confirmed diagnosis. Eyes were dilated and scans were acquired using the Zeiss Cirrus 5000 spectral domain OCT (SD-OCT) HD21 cube protocol. Therefore, 3D SD-OCT cubes consisted of 21 parallel 9 × 2 mm horizontal scans spaced 0.4 mm apart.

B. Image Processing and Data

Raw IMG data files were exported, converted to tiff file format and stored as 8-bit integer images, with a spatial resolution of 1024 × 1024 pixels. Each B-scan is a unit8 grayscale digital image comprised of 256 intensity levels. The B-scan is formed by successive axial scans (A-scans) at different transverse locations of retinal tissue. A stack of parallel B-scans as seen in Fig. 1 (A) are the constituents of the 3D SD-OCT cube depicted in Fig. 1 (C). Retinal contour was defined as the highly reflective retinal pigment epithelium (RPE) layer, marked in red in Fig. 1 (B). The scan axes are given in relation to the eye in Fig. 1 (D). Consequently, cube volume is defined as $V(X,Y,Z)$, were X denotes the primary scan direction, Y denotes the secondary scan direction and Z the axial scan direction. Cubic volume, V has average dimensions of $9 \times 8 \times 2$ mm^3.

III. Method

All 51 eyes were evaluated with both the LVW and GSF methods. Shape information was acquired from the same retinal images firstly using LVW and secondly the GSF. All image analyses were performed by a single user on a

T. Lange with College of Science and Engineering (tyra.lange@flinders.edu.au), S. Lake with College of Medicine and Public Health (srlake@gmail.com), K. Reynolds with College of Science and Engineering, Medical Device Research Institute (karen.reynolds@flinders.edu.au), M. Bottema with College of Science and Engineering (murk.bottema@flinders.edu.au), Flinders University, Adelaide, South Australia.

MacBook pro 2019 (2.4GHz, 32GB RAM). The GSF was implemented following pseudo code proposed by Chui et al. [9] and applied within the Graph-Based Segmentation software [4] using MATLAB software and the Image Processing Toolbox. Within both the LVW and GSF method, each image is represented as a graph (G) which is a data structure of sets of vertices (V) and edges (E), where each vertex corresponds to a pixel. Therefore, the image is represented as $G=(V,E)$. Where $e_{i,j}$ is an edge connecting a set of vertices or pixels v_i and v_j. A real number is assigned to an edge ($e_{i,j}$) within the graph and is termed its weight ($w_{i,j}$). Low weight values are assigned to vertex pairs with large vertical gradients. The graph is cut by determining the minimum weighted path that connects two endpoints using Dijkstra's algorithm and the RPE layer is successfully delineated. In the GSF weights are calculated via Eq. (1), where g_i denotes the vertical gradient of the image at pixel i and g_j denotes vertical gradient of the image at pixel j. The weights are given by:

$$w_{i,j} = 2 - (g_i + g_j) + w_{min} \quad (1)$$

where, w_{min} is the graph minimum weight (1×10^{-5}) included to improve stability. Both methods required user interaction with each B scan. For LVW, the contour was traced by the user from the start to end point and multiple mid-way marks were often necessary to guide contour identification. For GSF, the start and end points of each accurately identified section of retinal contour were manually marked. A best fit curve was extracted from the contour, with the residual irregularity converted to the frequency domain and compared to the average irregularity. This difference (anomaly) was tested with quadratic discriminant analysis, using anomaly frequency ranges of 0.11-0.33 cycles/mm. The two methods were compared by the category label ultimately attributed to each eye and the time required to generate results.

Time for each method was calculated using the final modification time in the file metadata, identified by the dir function in MATLAB. For Livewire, this was the sum of the time between first and last textfile created for each of the two OCT cubes that stored the contour information. This time includes only time taken to extract shape information. For GSF, the time between creation of the first tiff image file to the time of the last image analysis datafile saved was used. This time period includes conversion of .img file to .tif format, extraction of shape information, as well as classification.

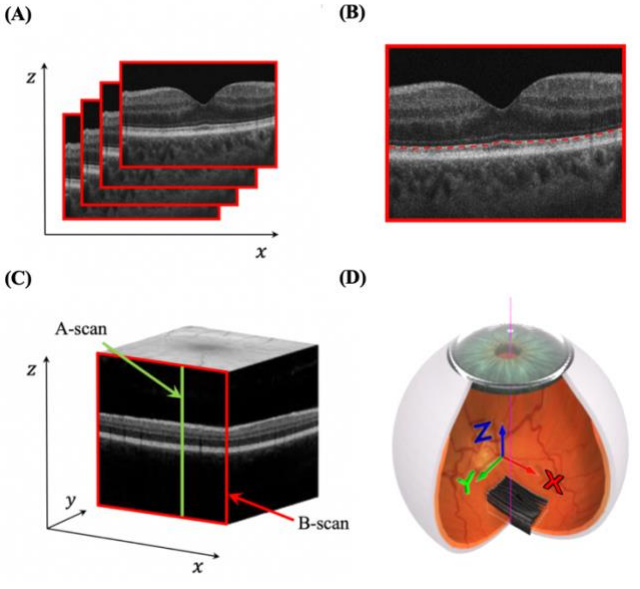

Fig. 1. Coordinate System in Retinal 3D SD-OCT Imaging [10, 11].

IV. Results

All 28 eyes with a known category were labelled the same with both LVW and GSF methods. Consequently, both methods diagnosed 28 eyes with PVD or RD correctly. 21 of 23 eyes in the predictive test group were given the same label with both methods. The root-mean-square error (RMSE) was used to calculate the average pixel distance between the two different segmentations methods. In the form mean (μ) ± standard deviation (SD), difference in pixel location between the two methods was 3.32 ± 1.25 pixels (n=51).

Outlying run times arose due to interrupted processing with both methods, therefore any run time greater than 30 minutes was excluded. This left 46 LVW and 50 GSF time periods. Shape extraction with LVW was significantly slower in comparison to extraction with GSF. In the form mean (μ) ± standard deviation (SD), LVW extraction took 814 ± 223 s, whereas GSF extraction took 524 ± 62 s ($p < 0.0005$). With longer processing times occurring with LVW in all but 4 of 45 eyes. Fig. 2 shows histograms of the processing time for the LVW method (A) and the GSF method (B).

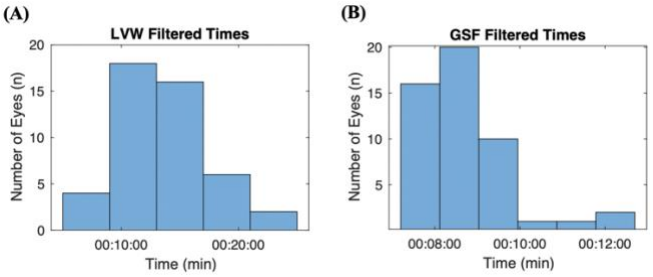

Fig. 2. Filtered Digital OCT Image Processing Times.

V. Discussion

Both the LVW and GSF accurately delineated retinal morphology. The LVW time included only time taken for retinal shape identification, and did not include the time for identifying the contour in the first B scan in each cube (as the start time was when the first B scan data was saved), whereas the GSF time included all B scans, classification time, and conversion of .img format image data files to tiff files. Despite these processing differences favouring the LVW method, LVW took significantly longer. The reduction in processing time of almost 5 minutes per eye is enough to make the GSF a practical point of care test in the clinical setting. Furthermore, user input is simplified with the GSF algorithm. increasing its acceptability.

VI. Conclusion

The GSF was faster than the LVW method in delineating retinal morphology, with the same accuracy. Such computational methods could be used as advanced diagnostic tools aimed at helping trained doctors in interpreting ocular abnormalities more accurately and instantly. Therefore, facilitating better patient diagnosis and prognosis. It is proposed that ophthalmic pathology be parametrised using this method to improve patient management. It will enable large-scale clinical studies into retinal shape. Ultimately, providing a quantified description of retinal shape for healthy and pathological eyes will help optimise and automate clinical diagnosis and improve clinical care.

REFERENCES

[1] D. Huang, E. A. Swanson, C. P. Lin, J. S. Schuman, W. G. Stinson, W. Chang, M. R. Hee, T. Flotte, K. Gregory, C. A. Puliafito, J. G. Fujimoto. 1991. 'Optical coherence tomography'. *Science*, 254 (5035). pp. 1178-1181. (New York, N.Y.)

[2] M. Sonka, M. D. Abràmoff. 2016. 'Quantitative Analysis of Retinal OCT'. *Medical Image Analysis*. pp. 165-169.

[3] M. Abramoff, M. K. Garvin, M. Sonka. 2010. 'Retinal imaging and image analysis'. *IEEE Rev Biomed Eng*, 20(3). pp. 169–208.

[4] P. Teng. 'Caserel–an open source software for computer-aided segmentation of retinal layers in optical coherence tomography images'. Zenodo. 2013;10. https://doi.org/10.5281/zenodo.17893.

[5] F. Rathke, S. Schmidt, C. Schnörr. 2014. 'Probabilistic Intra-retinal Layer Segmentation in 3-D OCT Images Using Global Shape Regularization'. *Medical Image Analysis*, 18(5). pp. 781-794.

[6] S. Naz, A. Ahmed, M. U. Akram, S. A. Khan. 2016. 'Automated Segmentation of RPE Layer for the Detection of Age Macular Degeneration Using OCT Images'. *2016 IEEE Sixth International Conference on Processing Theory, Tools and Applications.* pp. 1-4

[7] A. Yazdanpanah, G. Hamarneh, B. R. Smith, M. V. Sarunic. 2011. 'Segmentation of Intra-Retinal Layers From Optical Coherence Tomography Images Using an Active Contour Approach'. *IEEE Transactions on Medical Imaging*, vol. 30, no. 2. pp. 484-496.

[8] O. Perdomo, S. Otalora, F. A. Gonzalez, F. Meriaudeau, H. Muller. 2018. 'OCT-NET: A Convolutional Network for Automatic Classification of Normal and Diabetic Macular Edema Using Sd-oct Volumes'. *2018 IEEE 15th International Symposium on Biomedical Imaging (ISBI 2018)* 2018. pp. 1423-1426.

[9] S. J. Chiu, J. A. Izatt, R. V. O'Connell, K. P. Winter, C. A. Toth, S. Farsiu. 2012. 'Validated Automatic Segmentation of AMD Pathology including Drusen and Geographic Atrophy in SD-OCT Images'. *Investigative Ophthalmology, Science,* 53(1). pp. 53-61.

[10] L. De Sisternes, G. Jonna, J. Moss, M. F. Marmor, T. Leng, D. L. Rubin. 2017. 'Automated Intraretinal Segmentation of SD-OCT Images in Normal and Age-related Macular Degeneration Eyes'. *Biomedical Optics Express*, 8(3). pp. 1926-1949.

[11] J. Wu. 2017. 'Retinal Surface Prediction in Ophthalmic Spectral-Domain Optical Coherence Tomography'. *IEEE Transactions On Medical Imaging*, 24(8).